

available at www.sciencedirect.comwww.elsevier.com/locate/brainres

**BRAIN
RESEARCH**

Research Report
Zinquin identifies subcellular compartmentalization of zinc in cortical neurons. Relation to the trafficking of zinc and the mitochondrial compartment
Robert A. Colvin*, Meggan Laskowski, Charles P. Fontaine
Department of Biological Sciences, Program in Neuroscience, Ohio University, Athens, OH 45701, USA

ARTICLE INFO
Article history:

Accepted 7 February 2006

Available online 11 April 2006

Keywords:

Zinc sequestration

Primary cell culture

Fluorescence microscopy

Rat brain

Endosome

ABSTRACT

Zinquin (Zn^{2+} selective fluorophore), when used to visualize intracellular Zn^{2+} , typically shows brightly fluorescent perinuclear endosome-like structures, presumably identifying Zn^{2+} containing organelles. In this study, zinquin identified numerous and widespread sites of Zn^{2+} compartmentalization in primary cultures of embryonic rat cortical neurons. Nuclear fluorescence, however, was absent. We labeled neuronal mitochondria with MitoTracker Green in the presence of zinquin and show that the fluorescent patterns of MitoTracker Green and zinquin were distinct and clearly different in both the perinuclear region and in processes. The mitochondrial compartment was much larger than the sum of the areas of zinquin fluorescence, as indicated by the small amount (<10% MitoTracker Green over zinquin) of overlap of MitoTracker Green on zinquin. Zinquin fluorescence was unaffected by carbonyl cyanide 4-(trifluoromethoxy)phenylhydrazone (FCCP) treatment. The zinquin fluorescent objects were generally spherical in shape with a average diameter of about 0.6 μm . Most fluorescent objects, nearly two thirds on average, appeared to be docked, but both anterograde and retrograde movements were observed by time lapse image analysis. Although some fluorescent objects moved as much as 1 μm in 5 min, typical movements were smaller, usually 0.5 μm or less. Colchicine treatment caused striking aggregation of MitoTracker Green most noticeable in the perinuclear region. Zinquin fluorescence similarly showed reduced distribution throughout the cytoplasm, suggesting that zinquin fluorescent structures were associated with microtubules. Treatment with cytochalasin D had little noticeable effect on either the pattern of zinquin and MitoTracker Green fluorescence or their coincidence. Thus, numerous Zn^{2+} sequestering organelles/structures are present in perinuclear regions and processes of cultured neurons and are sometimes found coincident with mitochondria. We demonstrated real time trafficking of sequestered Zn^{2+} , using zinquin fluorescence, apparently associated with an endosome-like compartment or protein complexes in the cytosol.

© 2006 Elsevier B.V. All rights reserved.

* Corresponding author. Fax: +1 740 593 0300.

E-mail address: colvin@ohio.edu (R.A. Colvin).

1. Introduction

Zinquin, a Zn^{2+} selective fluorophore, has been used by many investigators in numerous mammalian cell types to visualize intracellular Zn^{2+} (Colvin et al., 2002; Haase and Beyersmann, 2002; Michalczyk et al., 2002; Ranaldi et al., 2002; Snitsarev et al., 2001; St Croi et al., 2002). The results of these studies typically show brightly fluorescent perinuclear endosome-like structures, presumably identifying Zn^{2+} containing organelles within the cytoplasm. Whereas the function of Zn^{2+} containing vacuoles in yeast is well defined (Devirgiliis et al., 2004; MacDiarmid et al., 2002; MacDiarmid et al., 2003), this is not the case for zinquin fluorescent structures found in mammalian cells. The goal of the present studies is to begin to characterize these structures in primary cultures of cortical neurons. Zinquin fluorescent structures are observed both in the soma and processes of cultured cortical neurons maintained in neurobasal media, suggesting that these structures have a role to play in normal Zn^{2+} homeostasis and trafficking (Colvin et al., 2002). In addition, these structures apparently accumulate significant Zn^{2+} when cells are under various stresses (Haase and Beyersmann, 1999, 2002; Pearce et al., 2000; Smith et al., 2002; St Croi et al., 2002; Tartler et al., 2000). Attempts to identify the transporters responsible for Zn^{2+} sequestration have met with mixed success (Kirschke and Huang, 2003; Michalczyk et al., 2002; Palmiter et al., 1996; Ranaldi et al., 2002).

The widespread distribution of zinquin fluorescence in cultured cortical neurons suggests that these structures could be associated with mitochondria. Many studies have shown a linkage between Zn^{2+} and mitochondrial function and dysfunction in cultured neurons. There is convincing evidence that when neuronal cytosolic concentrations of Zn^{2+} rise under pathological conditions, Zn^{2+} is taken up by mitochondria with derangements of mitochondrial structure and function (Dineley et al., 2003; Jiang et al., 2001; Sensi et al., 2003a, 2002, 1999, 2000; Wudarczyk et al., 1999). Such Zn^{2+} -dependent derangements in mitochondrial structure and function appear to contribute to cell death involving apoptotic pathways (Bossy-Wetzel et al., 2004; Budd et al., 2000). Thus, there is evidence for mitochondrial Zn^{2+} interactions under pathological conditions, but what is the evidence for the existence of endogenous Zn^{2+} in mitochondria that might be detectable by zinquin?

In elegant studies, from Sensi et al. (2003a), it was shown that RhodZin-3 (a Zn^{2+} selective fluorophore that accumulates in mitochondria) yields TPEN (tetrakis-(2-pyridylmethyl)ethylenediamine) sensitive punctate fluorescence in neurons. RhodZin-3 has a high affinity for Zn^{2+} (≈ 65 nM) suggesting that endogenous mitochondrial Zn^{2+} is in the nanomolar range (Sensi et al., 2003b). Recent studies (Malaiyandi et al., 2005) using isolated brain mitochondria have demonstrated pathways for the transport and accumulation of Zn^{2+} . In the present studies, we sought to find direct evidence to test the hypothesis that structures associated with zinquin fluorescence in cultured cortical neurons are associated with mitochondrial compartments. To accomplish this goal, we labeled neuronal mitochondria with the well characterized fluorophore MitoTracker Green in the presence of zinquin. To address the issue of Zn^{2+} trafficking in cultured cortical

neurons, we observed the real time movements of zinquin fluorescent objects by time lapse image analysis.

2. Results

2.1. The patterns of zinquin and MitoTracker Green fluorescence in living cortical neurons were distinct

Confocal microscopy improves horizontal and particularly vertical resolution of fluorescent images when compared with conventional epifluorescence. Unfortunately, in our studies, zinquin fluorescence showed very low intensity in living cells and required increasing the pinhole diameter to a point where the thickness of the optical section and image resolution was no better than conventional epifluorescence. Thus, we found that the best quality images were obtained using conventional epifluorescence equipped with a high resolution, high sensitivity, cooled CCD monochrome camera (see Experimental procedures). Although using this camera provided excellent images, we still had background fluorescence from out of focus structures complicating our image analysis. To remove out of focus fluorescence in our images, we used the flatten background feature of MetaMorph image analysis software (as detailed in the Experimental procedures) for postprocessing, resulting in still better quality, more informative images.

When cortical neurons grown and maintained in neurobasal media were coincubated with zinquin ester and MitoTracker Green and subsequently observed by conventional epifluorescence, characteristic and distinct patterns of fluorescence were observed (Fig. 1) for each fluorophore. Fig. 1 shows representative images of the perinuclear region (A–C) and a region of just processes (D–F). All neurons examined for MitoTracker Green showed a densely fluorescent perinuclear region, matching the well known distribution of mitochondria in this region of living neurons. Profiles of individual mitochondria were easily observed at any focal plane. This is shown in Fig. 1A. In Fig. 1D, only processes are shown and individual mitochondria are clearly distinguishable. Zinquin showed numerous fluorescent spots with minimal diffuse or background fluorescence in the perinuclear region. The nucleus was virtually devoid of zinquin fluorescence (Fig. 1B). Most processes showed a similar pattern of punctate zinquin fluorescence as was seen in the perinuclear region (Fig. 1E). Zinquin fluorescence under these conditions had previously been shown to be sensitive to the addition of tetrakis-(2-pyridylmethyl)ethylenediamine (TPEN), a membrane permeable metal chelator with high affinity for Zn^{2+} (Colvin et al., 2002). Also, when the neurons were exposed to 200 μM Zn^{2+} with 25 μM pyrithione (a Zn^{2+} ionophore), diffuse fluorescence in the cell body and nucleus increased dramatically (data not shown). Figs. 1C and F (perinuclear region and processes, respectively) show merged images of zinquin and MitoTracker Green fluorescence. Black arrows point to examples of regions where overlap occurred between the two fluorescent molecules, whereas white arrows point to examples of areas where zinquin fluorescence did not overlap with MitoTracker Green fluorescence. The fluorescent patterns of the two fluorophores were distinct and clearly different.

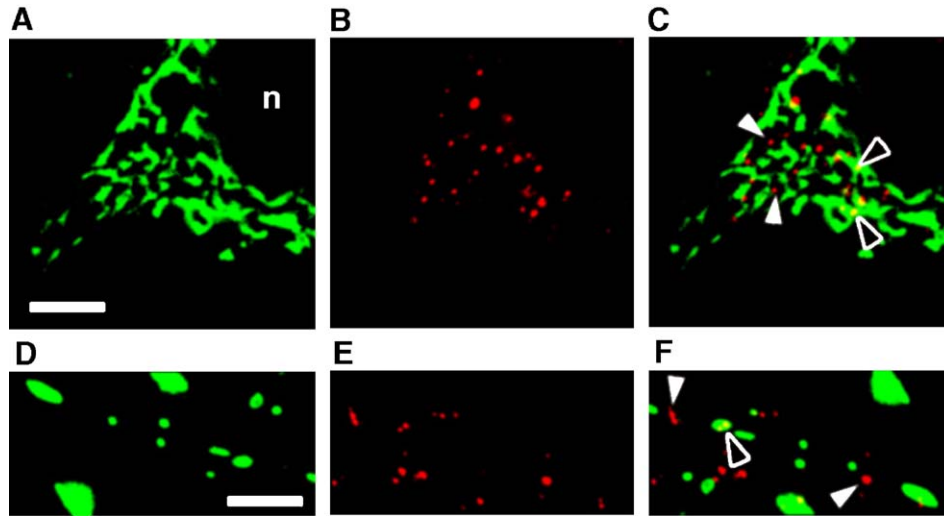


Fig. 1 – Zinquin (pseudo-colored red) and MitoTracker Green fluorescence observed in a living cortical neuron. Top row perinuclear region, bottom row processes. (A, D) MitoTracker Green fluorescence; (B, E) zinquin fluorescence; (C, F) merged images of panels A and B, or D and E, respectively. The white arrows point to examples of regions where zinquin fluorescence show no overlap with MitoTracker Green fluorescence, and black arrows point to examples of regions showing zinquin fluorescence overlap with MitoTracker Green fluorescence. Scale bar equals 5 μm . *n* = nucleus. (For interpretation of the references to colour in this figure legend, the reader is referred to the web version of this article.)

We used MetaMorph image analysis of paired images (zinquin and MitoTracker Green) to determine the relative size of the mitochondrial compartment compared to areas of zinquin fluorescence and to provide statistical evidence that the patterns of fluorescence illustrated in Fig. 1 were a consistent finding. Fig. 2 shows the results of overlap analysis using MetaMorph. The mitochondrial compartment was much larger than the sum of the areas of zinquin fluorescence. This was indicated by the small amount (generally less than 10%, see Fig. 2A, % MitoTracker over zinquin) of overlap of MitoTracker Green on zinquin. The amount of overlap of zinquin on MitoTracker Green was only about 20% (Fig. 2B, %

zinquin over MitoTracker Green), indicating that although MitoTracker Green and zinquin fluorescence were both widely distributed throughout both the perinuclear region and cell processes, the two fluorophores were probably not linked together or associated with each other, as such a condition would predict a high degree of overlap of zinquin on MitoTracker Green. Rather, it seems more likely that the overlap observed was random and merely the result of two distinct subcellular structures occupying neighboring cytoplasmic space. Thus, we concluded that because of the striking difference in size, shape, and distribution of the two fluorescent signals, the overlap represented two distinct

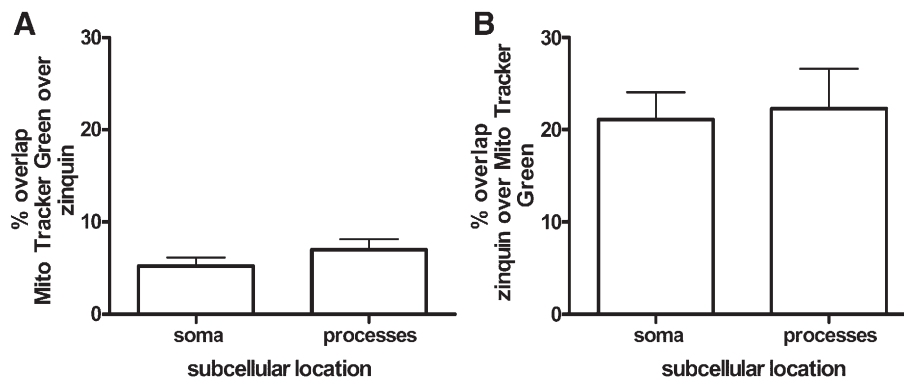


Fig. 2 – Results of fluorescence overlap analysis of zinquin and MitoTracker Green fluorescence. Digital images were analyzed using MetaMorph software (see Experimental procedures). Regions of interest were drawn around the appropriate cellular structures; cell body or processes in paired images of zinquin and MitoTracker Green fluorescence. Each bar represents the mean \pm SEM percent overlap between zinquin and MitoTracker Green fluorescence (A: MitoTracker Green over zinquin; B: zinquin over MitoTracker Green) in all images analyzed. *n* = 10 regions of interest containing one or more cells or processes. Data were obtained from three separate experiments. Neurons were incubated in neurobasal media throughout the experiment. No significant difference was seen when comparing means from soma and processes in either panel A or B.

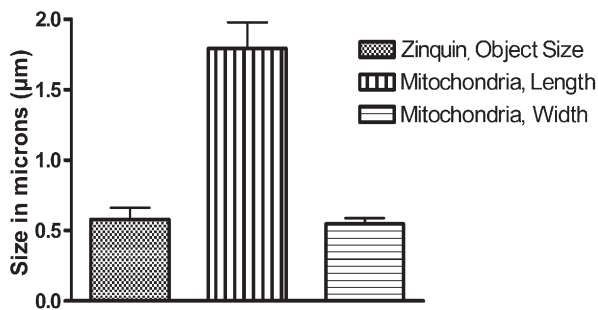


Fig. 3 – Digital images were analyzed for size using SPOT software. Lines were drawn across zinquin objects to measure diameter, or for mitochondria, lines were drawn that defined the length and width. $n =$ at least 12 objects. Each bar represents the mean \pm SEM of the measurements.

cellular structures with sometimes coinciding locations within the cell.

Next, we measured the apparent size of isolated mitochondria and zinquin fluorescent objects, both of which were easily resolved when associated with neuronal processes (Figs. 1D–F). Isolated mitochondria averaged about 2 μm in length and about 0.6 μm in width; sizes consistent with previous studies. The zinquin fluorescent objects were generally spherical in shape with an average diameter of about 0.6 μm (see Fig. 3). Size analysis of the zinquin objects was consistent with sizes usually given for endosomes.

2.2. Zinquin fluorescence was unaffected by addition of carbonyl cyanide 4-(trifluoromethoxy)phenylhydrazone (FCCP)

RhodZin-3 is a high affinity, highly selective Zn^{2+} fluorophore that preferentially distributes to mitochondria. It has been used to identify releasable intracellular stores of Zn^{2+} in neuronal mitochondria (Sensi et al., 2003a). Sensi et al. (2003a) showed that release of endogenous mitochondrial Zn^{2+} to the cytosolic compartment could be induced by the addition of FCCP. Thus, it was of interest to determine what effect FCCP would have on zinquin fluorescence. In control neurons, RhodZin-3 showed a pattern of fluorescence in both the perinuclear region and in processes that was nearly identical to that seen with MitoTracker Green (Fig. 4A, also seen in previous studies; Sensi et al., 2003a). After addition of 10 μM FCCP, mitochondrial specific fluorescence nearly disappeared (Fig. 4C). In contrast, zinquin fluorescence was unaffected by treatment with FCCP (Figs. 4B and D).

2.3. Disruption of microtubules caused a change in the pattern of both zinquin and MitoTracker Green fluorescence

Next, we determined what effect, if any, the disruption of the cytoskeleton would have on the pattern of zinquin fluorescence. One would expect that a Zn^{2+} containing structure found throughout the neuron would be associated with the cytoskeleton. We tested the effects of cytochalasin-D (disrupts microfilaments) and colchicine (disrupts microtubules) on MitoTracker Green and zinquin fluorescence. At the concen-

trations and incubation conditions used in this study, we observed that microtubules (using antibodies to α -tubulin) and microfilaments (using rhodamine phalloidin) were in fact disrupted (Figs. 5A–F). Microtubules showed a filamentous shape and were distributed throughout the soma (excluding the nucleus) and showed a parallel arrangement in processes (Figs. 5A and D). After treatment with colchicine, tubulin protein was aggregated and the filamentous distribution disappeared (Fig. 5B). Actin showed a uniform distribution (Figs. 5D and E) that was enriched near the plasma membrane. After treatment with cytochalasin D, actin proteins were aggregated and tended to accumulate in the perinuclear region (Fig. 5F). In addition, cytochalasin-D had no effect on microtubule structure (Fig. 5C) and colchicine likewise had no effect on microfilament structure (Fig. 5E).

Figs. 6A–D show that there was no discernible effect of cytochalasin-D pretreatment on the distribution of either fluorophore in either the perinuclear region or processes (compare with Fig. 1A–F). In contrast, colchicine treatment caused a striking condensation of MitoTracker Green fluorescence resulting in an encircling of the nucleus (Fig. 6G) in the perinuclear region and a similar “clumping” of fluorescence in the processes causing bulges to appear in the processes (Fig. 6J). The effect of colchicine treatment on zinquin fluorescence was less striking but still evident. The

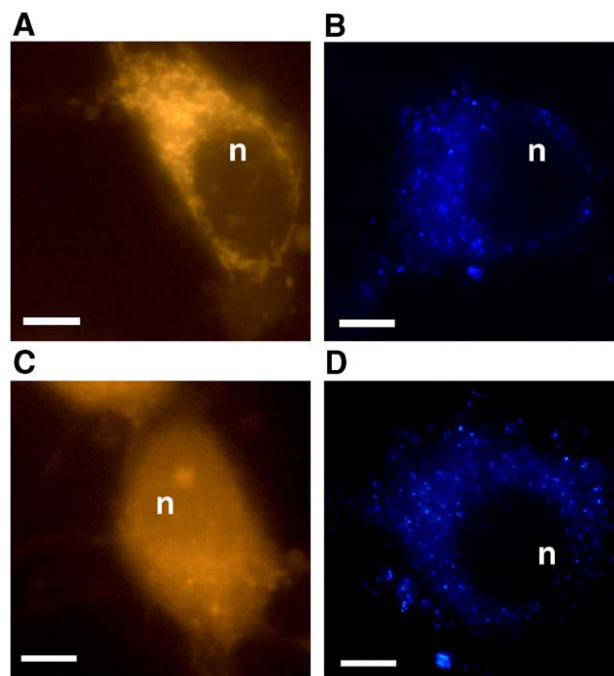


Fig. 4 – Neurons were preloaded with either zinquin or RhodZin-3 for 45 min at 37 $^{\circ}\text{C}$ (see Experimental procedures). The neurons were then washed in fresh neurobasal media. Next, the cells were incubated with 10 μM carbonyl cyanide 4-(trifluoromethoxy)phenylhydrazone (FCCP) for 5 min at 37 $^{\circ}\text{C}$. Images were obtained from cells while still exposed to FCCP. (A and C) RhodZin-3 fluorescence; (B and D) zinquin fluorescence; (A and B) control; (C and D) after addition of FCCP. Images are representative of results obtained in three separate experiments. Scale bar equals 5 μm .

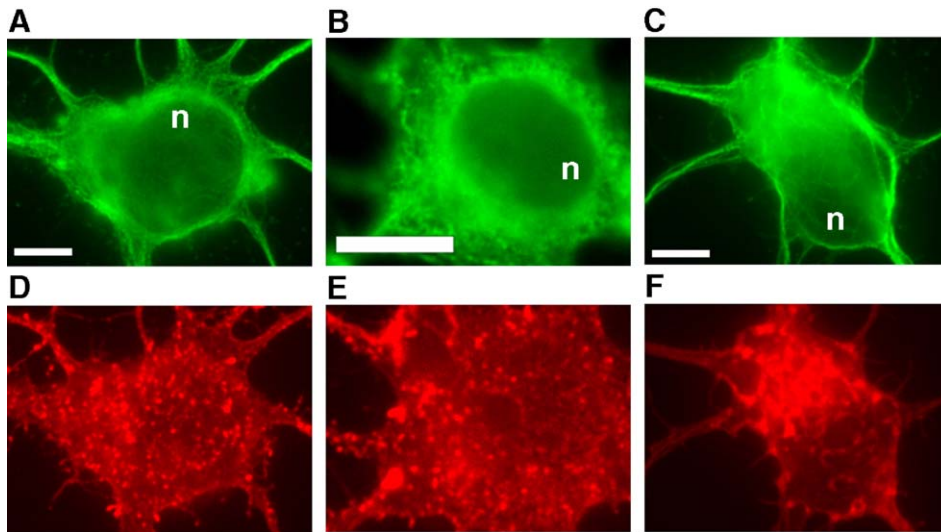


Fig. 5 – The neuron pictured in panels A and D was exposed to control conditions, incubated in neurobasal throughout. The neuron pictured in panels B and E was incubated in colchicine 30 $\mu\text{g/ml}$ for 4 h at 37 $^{\circ}\text{C}$, and the neuron pictured in panels C and F was incubated in cytochalasin D 10 $\mu\text{g/ml}$ for 5 h at 37 $^{\circ}\text{C}$. Neurons were fixed and immunostained as described in Experimental procedures. Neurons in panels A–C were incubated with 1:2000 anti α tubulin (mouse monoclonal IgG) for 1 h at room temperature, then 1:2000 Alexa-488 anti-mouse (Molecular Probes) for 1 h at room temperature. Neurons in panels D–F were incubated with 1:25 phalloidin AF-546 (Molecular Probes) for 1 h at room temperature. Images are representative of results obtained in three separate experiments. Scale bar equals 5 μm .

zinquin fluorescence tended towards a more restricted pattern around the nucleus with some clumping in the processes (Figs. 6H and K). Figs. 6I and L are the corresponding merged images. Again, it is evident that the pattern of the two fluorophores is distinctly different in these images. The differing response of the two fluorophores to the colchicine pretreatment provides additional evidence that distinct cellular structures are identified by each fluorophore. The “clumping” of mitochondria along the processes after colchicine pretreatment is no doubt the result of the disruption of axonal transport of these organelles mediated at least in part by disruption of microtubules. Cellular structures identified by zinquin showed “clumping” as well (albeit not as severe as MitoTracker Green), suggesting that these structures are transported along microtubules too, and thus could be involved in the cellular trafficking of Zn^{2+} . “Clumping” of cellular structures identified by zinquin occurred at the same locations that showed “clumping” of mitochondria (see black arrow, Fig. 6L).

2.4. Characteristics of zinquin object movements

To provide additional evidence for the role that zinquin objects might play in cellular Zn^{2+} trafficking, we observed the pattern of movement in paired images captured 5 min apart. Both anterograde and retrograde movements were observed, no preference for one type of movement over the other was noted. Movements were observed both in the processes and in the cell body. Although some objects moved as much as 1 μm in 5 min, the more typical movement was much smaller, 0.5 μm or less (Fig. 7). Since we used a linear analysis of movements, these values are likely to underes-

timate to some degree the true extent of movement. Most objects, nearly two thirds on average, appeared to be docked, as they showed no identifiable movements in the 5 min time frame (compare Figs. 8D and E). Although longer time lapse imaging was attempted, the movements of zinquin objects rapidly diminished with time. We attributed this to phototoxicity caused by UV light exposure. Thus, the large proportion of objects which were docked could partly be due to phototoxicity. This finding was also observed for mitochondrial movements; however, mitochondria generally moved much greater distances initially than did zinquin objects (compare Figs. 8B–E).

3. Discussion

Zn^{2+} is an essential trace element and the neurological consequences of dietary Zn^{2+} deficiency are well studied and characterized (for review, see Colvin et al., 2003). Some of the well described biochemical functions of Zn^{2+} in neurons as well as most cells, include a structural role in Zn^{2+} finger domains of DNA binding proteins and as a necessary cofactor of many enzymes (e.g., Cu^{2+} , Zn^{2+} superoxide dismutase). Zinc-enriched neurons are found in association with both excitatory (glutamatergic) and inhibitory (GABAergic) pathways, the highest density of which is found in the telencephalon. Zn^{2+} is well known to be colocalized with glutamate in the synaptic vesicles of excitatory terminals and is thought to be released along with neurotransmitter. In the brain, both extracellular and intracellular free Zn^{2+} ions are thought to have important signaling functions, such as modulation of GABAergic and

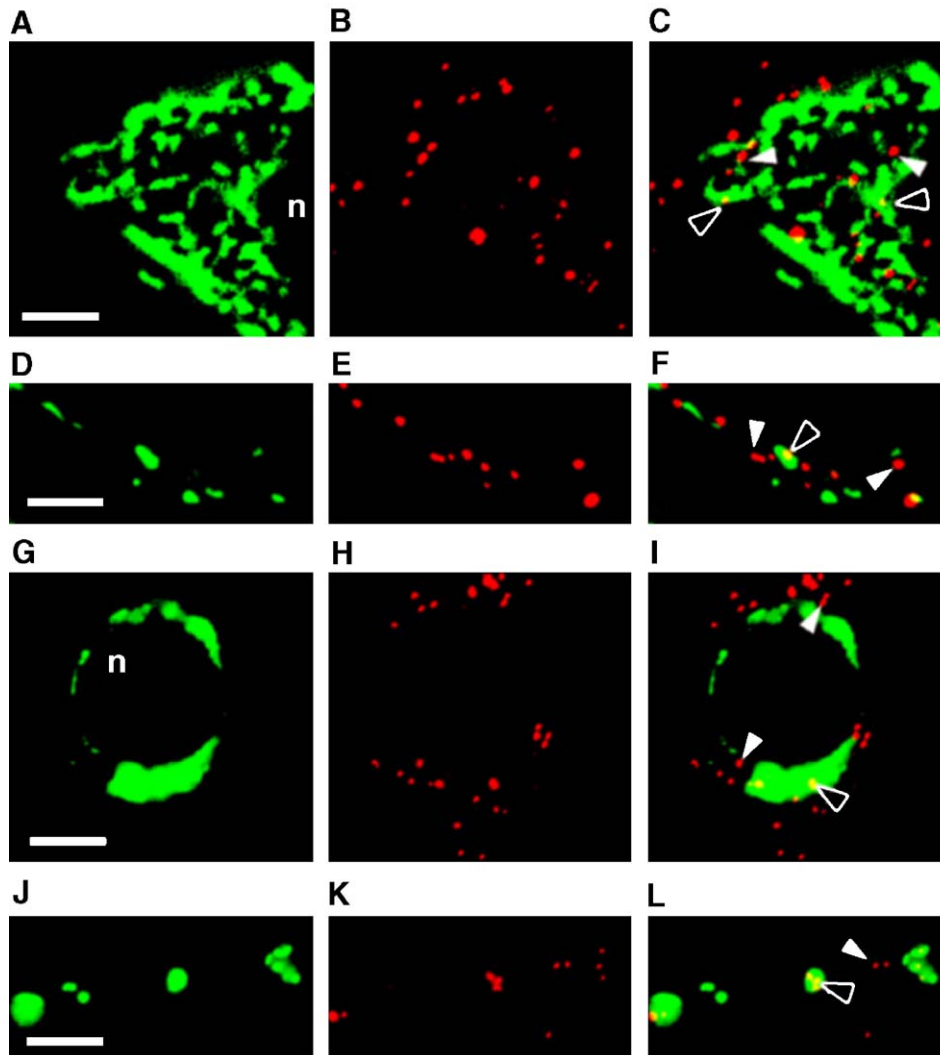


Fig. 6 – Zinquin (pseudo-colored red) and MitoTracker Green fluorescence observed in living cortical neurons after cytochalasin D (A–F) or colchicine (G–L) treatment. (A–C and G–I) Perinuclear region; (D–F and J–L) processes. (A, D, G, and J) MitoTracker Green fluorescence; (B, E, H, and K) zinquin fluorescence; (C, F, I, and L) merged images. The white arrows point to examples of regions where zinquin fluorescence shows no overlap with MitoTracker Green fluorescence, and black arrows point to examples of regions showing zinquin fluorescence overlap with MitoTracker Green fluorescence. Scale bar equals 5 μm . *n* = nucleus. Images are representative of results obtained in three separate experiments. (For interpretation of the references to colour in this figure legend, the reader is referred to the web version of this article.)

glutamatergic neurotransmission or modulation of protein kinase C signaling pathways.

The most important findings of this study are: (1) Zn^{2+} containing subcellular structures in living cortical neurons have a widespread distribution but are not mitochondria and (2) some of the structures identified by zinquin fluorescence were observed moving within cortical neurons. But what are these structures? It is now well established that the synaptic vesicles of glutamatergic neurons contain significant amounts of Zn^{2+} (Cole et al., 1999; Frederickson et al., 2005; Salazar et al., 2004). We used low density cultures in the present studies, therefore, synaptic connections are sparse such that presynaptic vesicles could not account for the number and distribution of zinquin fluorescent structures we observed. Some of the cellular structures identified by

zinquin fluorescence in cell bodies and processes could be maturing synaptic vesicles, moving towards their eventual destination at the synapse. However, it is well established that Zn^{2+} in maturing vesicles, either in the cell body or axon, is not histochemically reactive (Frederickson et al., 1989), *in vivo*. Since the fluorescent zinquin objects were not mitochondria and it seems unlikely that synaptic vesicles could account for their diffuse distribution in cultured neurons, we propose that these objects represent an endosome-like compartment involved in the sequestration of intracellular Zn^{2+} . Several studies have now described the subcellular distribution of Zn^{2+} transporters of both the SLC30 (ZnT) and SLC39 (ZIP) families in the trans-golgi network (Chimienti et al., 2005; Huang et al., 2002; Huang et al., 2005; Kirschke and Huang, 2003). Thus, a mechanism

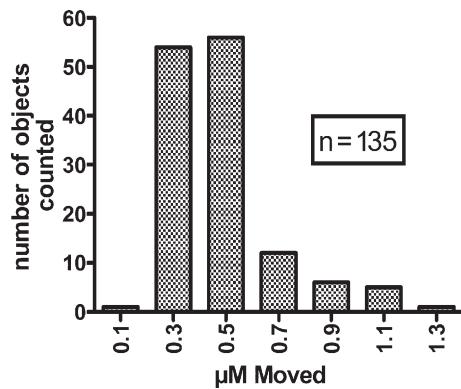


Fig. 7 – A frequency distribution showing the distribution of movement distances in 5 min, recorded for 135 separate objects from six different coverslips. The size of each bin is 0.2 μm .

exists for the import and export of Zn^{2+} from these compartments. It appears certain that Zn^{2+} associated with this compartment is involved with the incorporation of Zn^{2+} into maturing proteins that require Zn^{2+} as a necessary structural or functional cofactor. In addition, experimental evidence suggests that an endosome-like compartment is involved in the sequestration of excess intracellular Zn^{2+} in a wide variety of cells. When cells are Zn^{2+} stressed or under oxidative conditions and Zn^{2+} is released from metallothionein, intracellular “free” Zn^{2+} levels rise significantly. Under these conditions, fluorophores like zinquin yield a diffuse fluorescence that includes the nucleus. Previous studies in cells other than neurons have shown that the fluorescent intensity of structures identified by zinquin increases considerably when cells are stressed (Haase and Beyersmann, 1999, 2002; Smith et al., 2002; St Croi et al., 2002; Tang et al., 2001). We showed that Zn^{2+} was not released from these structures when neurons were exposed to FCCP. Thus, sequestration was not dependent on membrane potential or proton gradients. Cellular structures identified by zinquin could be membrane delimited as discussed above, but also could represent cytosolic protein complexes that contain significant amounts of Zn^{2+} . These complexes could contain various Zn^{2+} binding proteins, including metallothionein and could provide a mechanism for trafficking and exchanging Zn^{2+} between various Zn^{2+} containing proteins within the cell. Based on the affinity of many cytosolic Zn^{2+} binding proteins including metallothionein (stability constant = 10^{-12} M), it seems most likely that “free” intracellular Zn^{2+} in quiescent cells is very low. Therefore, it is not surprising that zinquin does not detect intracellular “free” Zn^{2+} in resting neurons. Thus, cells require a mechanism for shuttling Zn^{2+} to and fro between organelles and Zn^{2+} binding proteins. Freely diffusible protein clusters containing metallothionein could serve such a purpose. Although metallothionein has a very high affinity for Zn^{2+} , it has been shown that many proteins (e.g., glutathione disulfide) can act as releasing factors and mobilize Zn^{2+} from metallothionein (Jacob et al., 1998). In this respect, it is interesting to note that in vitro studies show that zinquin can scavenge Zn^{2+} from metallothionein (Coyle et al., 1994),

the implication being that zinquin would recognize Zn^{2+} bound to metallothionein containing protein clusters in the cytoplasm.

Finally, we propose that Zn^{2+} containing structures identified by zinquin are involved in the cellular trafficking of Zn^{2+} . We came to this conclusion based on the following

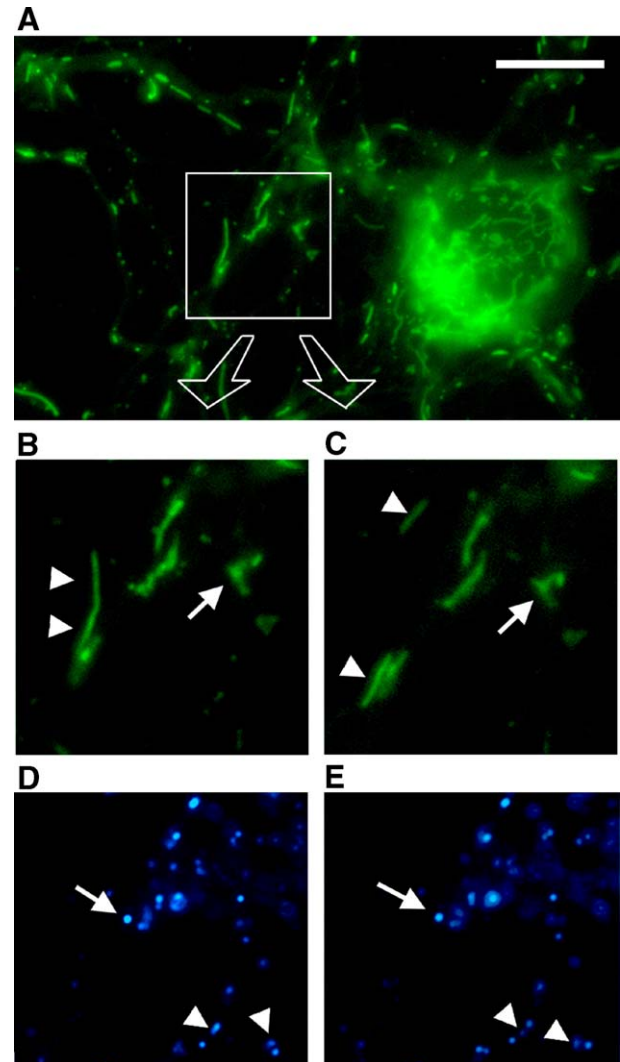


Fig. 8 – (A) Representative fluorescent image of cortical neurons pretreated with MitoTracker Green (0 time image capture). White outline is typical of a region of interest used for analysis of zinquin object movement. Scale bar equals 10 μm . (B) Region of interest shown in panel A for MitoTracker Green fluorescence, image captured at 0 time; (C) same region of interest as shown in panel B except image captured 5 min later. (D) Region of interest shown in panel A for zinquin fluorescence, image captured at 0 time; (E) same region of interest as shown in panel D except image captured 5 min later. Arrowheads without tails point to mitochondria/zinquin objects that were docked and did not move during the 5 min interval; arrowheads with tails point to mitochondria/zinquin objects that did move during the same 5 min interval. (For interpretation of the references to colour in this figure legend, the reader is referred to the web version of this article.)

experimental observations: (1) the structures contained Zn²⁺ as evidenced by zinquin fluorescence and were present in normal healthy cultured cortical neurons, (2) the widespread cellular distribution of such structures, (3) their distribution in the cell was altered when microtubule structure was disrupted, and finally, (4) observations that these structures move about in the cell body and travel along neuronal processes in both the retrograde and anterograde direction.

4. Experimental procedures

4.1. Cell culture

Primary culture of embryonic (E-18) Sprague–Dawley rat cortical neurons was performed as described previously (Colvin et al., 2002). Briefly, brains are removed from the skulls and kept moist in Hank's balanced saline solution (without Mg²⁺ and Ca²⁺) (HBSS) for further dissection. Using a dissecting microscope, the cerebral cortex was carefully separated, using blunt dissection, from the brainstem, diencephalon, olfactory bulbs, and cerebellum, which were discarded. Next the meninges and choroid plexus were stripped away. The cerebral hemispheres were cut into small pieces (about four pieces for each hemisphere) and trypsinized in HBSS at room temperature. After trypsinization, nerve cells were dissociated by gentle trituration through the narrow opening of a fire polished Pasteur pipette. The dissociated neurons suspended in HBSS were added to 24 well culture plates (Falcon) containing sterilized 12 mm no. 1 glass coverslips coated with polyethylenimine (50% solution, Sigma, St. Louis, MO, USA), which was diluted 1:1000 in borate buffer. The cortical neurons are allowed to attach to the surface at 37 °C, 5% CO₂ in 0.5 ml of MEM solution (Gibco BRL) supplemented with 10 mM sodium bicarbonate, 2 mM L-glutamate, 1 mM pyruvate, 20 mM KCl and 10% (v/v) heat inactivated fetal bovine serum. After 3 to 6 h, the media were replaced with fresh supplemented MEM and 24 h later switched to neurobasal media (Gibco BRL) supplemented with 0.5 mM glutamine and 2% B27 (Gibco BRL). When these cultures were stained with glial fibrillary acidic protein, positive cells accounted for less than 10% of the cell population even without using mitotic inhibitors (data not shown). Free Zn²⁺ concentration in supplemented neurobasal media was 1.0 nM determined using a pZn meter supplied by Zinc Tools Inc. (<http://www.zinctools.com>).

4.2. Fluorescence microscopy

The cells grown on the coverslips were washed with fresh neurobasal media. The cells were then incubated for 45 min at 37 °C with either 50 nM MitoTracker Green or 1 μM RhodZin-3 (Molecular Probes, Eugene, OR) and/or 25 μM zinquin ester (Luminus, Adelaide, SA, Australia). Cells were washed once in neurobasal media before placing in a heated (37 °C), closed perfusion chamber (Warner Inst., model RC-30HV) filled with neurobasal media. Cells were examined using conventional epifluorescence (Nikon, Diaphot 300) equipped with a Nikon 100×, 1.4 NA Plan Apo oil-immersion objective. For Mito-

Tracker Green, the FITC-HYQ filter sets were used; for zinquin the UV-2E/C DAPI filter sets were used; and for RhodZin-3 the TRITC (Rhodamine) Dil filter sets were used (Chroma, Rockingham, VT).

4.3. Image capture and analysis

Fluorescent images were captured with a cooled CCD camera (Spot, RT ES, model 9.1 Monochrome w/IR-6). Paired images were opened in the MetaMorph software suite (ver. 4.6r5, Universal Imaging, West Chester, PA), background fluorescence levels were reduced with the flatten background tool and images thresholded manually. Regions of interest were then drawn around the appropriate cellular structures; cell body or processes. Colocalization within the thresholded regions of interest was determined with the measure colocalization tool. The data are presented as the percentage of MitoTracker Green fluorescence over zinquin fluorescence as well as zinquin over MitoTracker Green. Images shown in figures were pseudo-colored with the Spot software as appropriate and saved separately from the monochromatic data. The relevant foreground data were separated from background fluorescence with the adjust histogram tool. The images, MitoTracker Green and zinquin, were then merged with the merge image tool.

4.4. Size analysis

To measure the fluorescent object size, regions of interest were chosen in representative images. The Spot software (ver 4.1.1, Diagnostic Instruments Inc.) add measurement feature was used to measure the objects. Using this feature, a straight line was drawn defining the diameter of the spherical zinquin objects or the length and width of mitochondria. Pixel length of each line was determined and size determined by comparison to a calibration scale for the objective used.

4.5. Treatment with colchicine or cytochalasin D

Cells were treated with colchicine 30 μg/ml or cytochalasin D 10 μg/ml (Sigma, St. Louis, MO) in neurobasal media at 37 °C for 4 or 5 h, respectively. Cells were then washed once in neurobasal media before proceeding with the rest of the experiment as described above.

4.6. Methods used for immunofluorescence

Cortical neurons, attached to coverslips maintained in neurobasal media and/or treated with colchicine or cytochalasin D as described above, were fixed in phosphate-buffered saline (PBS) (Sigma), pH 7.4, containing 4% para-formaldehyde (Fisher) for 8 min at room temperature. The cells were then permeabilized in 0.1% Triton X-100 (Sigma) in PBS for 1 min at room temperature. Then, neurons were incubated with 1:2000 anti-α-tubulin antibody (mouse monoclonal IgG) in Bovine Serum Albumin (Sigma) with 5% Normal Goat Serum (Gibco) (BSA/NGS) for 1 h at room temperature. The coverslips were rinsed three times through PBS then treated with 1:2000 Alexa-488 anti-mouse (Molecular Probes) and 1:25 phalloidin AF-546 (Molecular Probes) in BSA/NGS for 1 h at room

temperature in the dark. The coverslips were finally rinsed three times through PBS and all were mounted on glass microscope slides (VWR) using 6.5 μ l Anti-Fade reagent (Molecular Probes).

4.7. Recording and measurement of zinquin object movements

Cells were preincubated with zinquin and MitoTracker Green and movements were recorded using the same conditions/objective as described above for fluorescence microscopy. Conditions were designed to reduce light exposure, thus reducing phototoxicity. To that end, an ND2 filter was placed in the light path and the shutter was closed except when capturing an image. A field was selected and correct focus determined using MitoTracker Green fluorescence. Next, two images (one for each filter set) of the same field of neurons were captured (typically 200–300 ms exposure time each) and 5 min later the same procedure was repeated, capturing two new images. The zinquin image corresponding to the 5 min time increment was pseudo-colored red. Thus, the zinquin objects that had not moved appeared purple and those that had moved showed two spots, a blue spot at its location in the 0 time image and a red spot at the 5 min location. Within a region of interest, zinquin objects were counted and tabulated as those that had moved and those that did not move. For those objects that did move, a travel distance was measured using the SPOT software add measurement feature. A straight line was drawn between the centers of each pair of zinquin objects that had moved. The length of that line was determined as described in size analysis (see above).

4.8. Statistical analysis of fluorescence overlap

Data were derived from at least three replicate experiments (coverslips). At least 10 regions of interest were selected from the digital images collected for overlap and size analysis. Data are presented as mean \pm SEM of all 10 analyses. Combined data were analyzed by one-way ANOVA followed by Tukey's multiple comparison test. Differences in the means were judged significant when $P < 0.05$.

Acknowledgments

This work was supported by a grant from the National Institute on Aging and the Provost's Undergraduate Research Fund at OHIO University.

REFERENCES

- Bossy-Wetzel, E., Talantova, M.V., Lee, W.D., Scholzke, M.N., Harrop, A., Mathews, E., Gotz, T., Han, J., Ellisman, M.H., Perkins, G.A., Lipton, S.A., 2004. Crosstalk between nitric oxide and zinc pathways to neuronal cell death involving mitochondrial dysfunction and p38-activated K^+ channels. *Neuron* 41, 351–365.
- Budd, S.L., Tenneti, L., Lishnak, T., Lipton, S.A., 2000. Mitochondrial and extramitochondrial apoptotic signaling pathways in cerebrocortical neurons. *Proc. Natl. Acad. Sci. U. S. A.* 97, 6161–6166.
- Chimienti, F., Favier, A., Seve, M., 2005. ZnT-8, a pancreatic beta-cell-specific zinc transporter. *Biometals* 18, 313–317.
- Cole, T.B., Wenzel, H.J., Kafer, K.E., Schwartzkroin, P.A., Palmiter, R. D., 1999. Elimination of zinc from synaptic vesicles in the intact mouse brain by disruption of the ZnT3 gene. *Proc. Natl. Acad. Sci. U. S. A.* 96, 1716–1721.
- Colvin, R.A., 2002. pH dependence and compartmentalization of zinc transported across plasma membrane of rat cortical neurons. *Am. J. Physiol.: Cell Physiol.* 282, C317–C329.
- Colvin, R.A., Fontaine, C.P., Laskowski, M., Thomas, D., 2003. Zn²⁺ transporters and Zn²⁺ homeostasis in neurons. *Eur. J. Pharmacol.* 479, 171–185.
- Coyle, P., Zalewski, P.D., Philcox, J.C., Forbes, I.J., Ward, A.D., Lincoln, S.F., Mahadevan, I., Rofe, A.M., 1994. Measurement of zinc in hepatocytes by using a fluorescent probe, zinquin: relationship to metallothionein and intracellular zinc. *Biochem. J.* 303 (Pt 3), 781–786.
- Devirgiliis, C., Murgia, C., Danscher, G., Perozzi, G., 2004. Exchangeable zinc ions transiently accumulate in a vesicular compartment in the yeast *Saccharomyces cerevisiae*. *Biochem. Biophys. Res. Commun.* 323, 58–64.
- Dineley, K.E., Votyakova, T.V., Reynolds, I.J., 2003. Zinc inhibition of cellular energy production: implications for mitochondria and neurodegeneration. *J. Neurochem.* 85, 563–570.
- Frederickson, C.J., 1989. Neurobiology of zinc and zinc-containing neurons. *Int. Rev. Neurobiol.* 31, 145–238.
- Frederickson, Christopher J., Koh, Jae-Young, Bush, Asley I., 2005. The neurobiology of zinc in health and disease. *Nat. Rev., Neurosci.* 6, 449–462.
- Haase, H., Beyersmann, D., 1999. Uptake and intracellular distribution of labile and total Zn(II) in C6 rat glioma cells investigated with fluorescent probes and atomic absorption. *Biometals* 12, 247–254.
- Haase, H., Beyersmann, D., 2002. Intracellular zinc distribution and transport in C6 rat glioma cells. *Biochem. Biophys. Res. Commun.* 296, 923–928.
- Huang, L., Kirschke, C.P., Gitschier, J., 2002. Functional characterization of a novel mammalian zinc transporter, ZnT6. *J. Biol. Chem.* 277, 26389–26395.
- Huang, Liping, Kirschke, Catherine P., Zhang, Yunfan, Yan Yu, Yu, 2005. The ZIP7 Gene (Slc39a7) encodes a zinc transporter involved in zinc homeostasis of the golgi apparatus. *J. Biol. Chem.* 280 (15), 15456–15463.
- Jacob, C., Maret, W., Vallee, B.L., 1998. Control of zinc transfer between thionein, metallothionein, and zinc proteins. *Proc. Natl. Acad. Sci. U. S. A.* 95, 3489–3494.
- Jiang, D., Sullivan, P.G., Sensi, S.L., Steward, O., Weiss, J.H., 2001. Zn (2+) induces permeability transition pore opening and release of pro-apoptotic peptides from neuronal mitochondria. *J. Biol. Chem.* 276, 47524–47529.
- Kirschke, C.P., Huang, L., 2003. ZnT7, a novel mammalian transporter, accumulates zinc in the golgi apparatus. *J. Biol. Chem.* 278, 4096–4102.
- MacDiarmid, C.W., Milanick, M.A., Eide, D.J., 2002. Biochemical properties of vacuolar zinc transport systems of *Saccharomyces cerevisiae*. *J. Biol. Chem.* 277, 39187–39194.
- MacDiarmid, C.W., Milanick, M.A., Eide, D.J., 2003. Induction of the ZRC1 metal tolerance gene in zinc-limited yeast confers resistance to zinc shock. *J. Biol. Chem.* 278, 15065–15072.
- Malaiyandi, L.M., Vergun, O., Dineley, K.E., Reynolds, I.J., 2005. Direct visualization of mitochondrial zinc accumulation reveals uniporter-dependent and -independent transport mechanisms. *J. Neurochem.* 93, 1242–1250.
- Michalczyk, A.A., Allen, J., Blomeley, R.C., Ackland, M.L., 2002. Constitutive expression of hZnT4 zinc transporter in human breast epithelial cells. *Biochem. J.* 364, 105–113.

- Palmiter, R.D., Cole, T.B., Findley, S.D., 1996. ZnT-2, a mammalian protein that confers resistance to zinc by facilitating vesicular sequestration. *EMBO J.* 15, 1784–1791.
- Pearce, L.L., Wasserloos, K., St Croix, C.M., Gandle, R., Levitan, E.S., Pitt, B.R., 2000. Metallothionein, nitric oxide and zinc homeostasis in vascular endothelial cells. *J. Nutr.* 130, 1467S–1470S.
- Ranaldi, G., Perozzi, G., Truong-Tran, A., Zalewski, P., Murgia, C., 2002. Intracellular distribution of labile Zn(II) and zinc transporter expression in kidney and MDCK cells. *Am. J. Physiol.: Renal. Physiol.* 283, F1365–F1375.
- Salazar, G., Love, R., Werner, E., Doucette, M.M., Cheng, S., Levey, A., Faundez, V., 2004. The zinc transporter ZnT3 interacts with AP-3 and it is preferentially targeted to a distinct synaptic vesicle subpopulation. *Mol. Biol. Cell* 15, 575–587.
- Sensi, S.L., Yin, H.Z., Carriedo, S.G., Rao, S.S., Weiss, J.H., 1999. Preferential Zn²⁺ influx through Ca²⁺-permeable AMPA/kainate channels triggers prolonged mitochondrial superoxide production. *Proc. Natl. Acad. Sci. U. S. A.* 96, 2414–2419.
- Sensi, S.L., Yin, H.Z., Weiss, J.H., 2000. AMPA/kainate receptor-triggered Zn²⁺ entry into cortical neurons induces mitochondrial Zn²⁺ uptake and persistent mitochondrial dysfunction. *Eur. J. Neurosci.* 12, 3813–3818.
- Sensi, S.L., Ton-That, D., Weiss, J.H., 2002. Mitochondrial sequestration and Ca(2+)-dependent release of cytosolic Zn(2+) loads in cortical neurons. *Neurobiol. Dis.* 10, 100–108.
- Sensi, S.L., Ton-That, D., Sullivan, P.G., Jonas, E.A., Gee, K.R., Kaczmarek, L.K., Weiss, J.H., 2003a. Modulation of mitochondrial function by endogenous Zn²⁺ pools. *Proc. Natl. Acad. Sci. U. S. A.* 100, 6157–6162.
- Sensi, S.L., Ton-That, D., Weiss, J.H., Rothe, A., Gee, K.R., 2003b. A new mitochondrial fluorescent zinc sensor. *Cell Calcium* 34, 281–284.
- Smith, P.J., Wiltshire, M., Davies, S., Chin, S.F., Campbell, A.K., Errington, R.J., 2002. DNA damage-induced Zn(2+) transients: correlation with cell cycle arrest and apoptosis in lymphoma cells. *Am. J. Physiol.: Cell Physiol.* 283, C609–C622.
- Snitsarev, V., Budde, T., Stricker, T.P., Cox, J.M., Krupa, D.J., Geng, L., Kay, A.R., 2001. Fluorescent detection of Zn(2+)-rich vesicles with Zinquin: mechanism of action in lipid environments. *Biophys. J.* 80, 1538–1546.
- St Croix, C.M., Wasserloos, K.J., Dineley, K.E., Reynolds, I.J., Levitan, E.S., Pitt, B.R., 2002. Nitric oxide-induced changes in intracellular zinc homeostasis are mediated by metallothionein/thionein. *Am. J. Physiol.: Lung Cell. Mol. Physiol.* 282, L185–L192.
- Tang, Z.L., Wasserloos, K., St Croix, C.M., Pitt, B.R., 2001. Role of zinc in pulmonary endothelial cell response to oxidative stress. *Am. J. Physiol.: Lung Cell. Mol. Physiol.* 281, L243–L249.
- Tartler, U., Kroncke, K.D., Meyer, K.L., Suschek, C.V., Kolb-Bachofen, V., 2000. Nitric oxide interferes with islet cell zinc homeostasis. *Nitric Oxide* 4, 609–614.
- Wudarczyk, J., Debska, G., Lenartowicz, E., 1999. Zinc as an inducer of the membrane permeability transition in rat liver mitochondria. *Arch. Biochem. Biophys.* 363, 1–8.